



Research Article

# Parathyroid hormone promotes the osteogenesis of lipopolysaccharide-induced human bone marrow mesenchymal stem cells through the JNK MAPK pathway

 Ziyue Qin<sup>1,2,3,\*</sup>, Shu Hua<sup>2,3,4,\*</sup>, Huifen Chen<sup>2,3,5</sup>, Zhuo Wang<sup>2,3,6</sup>, Haoran Wang<sup>2,3,6</sup>, Jiamin Xu<sup>2,3,6</sup>,  
 Yuli Wang<sup>2,3,6</sup>, Wu Chen<sup>1,2,3</sup> and Weina Zhou<sup>2,3,4</sup>

<sup>1</sup>Department of Periodontology, The Affiliated Stomatological Hospital of Nanjing Medical University, Nanjing, China; <sup>2</sup>Jiangsu Province Key Laboratory of Oral Diseases, Nanjing Medical University, Nanjing, China; <sup>3</sup>Jiangsu Province Engineering Research Center of Stomatological Translational Medicine, Nanjing, China; <sup>4</sup>Department of Temporomandibular Joint, The Affiliated Stomatological Hospital of Nanjing Medical University, Nanjing, China; <sup>5</sup>Department of Endodontics, The Affiliated Stomatological Hospital of Nanjing Medical University, Nanjing, China; <sup>6</sup>Department of Oral and Maxillofacial Surgery, The Affiliated Stomatological Hospital of Nanjing Medical University, Nanjing, China

**Correspondence:** Yuli Wang (njykdwy@njmu.edu.cn) or Wu Chen (chenwu@njmu.edu.cn) or Weina Zhou (36408723@qq.com)



Periodontitis is a series of inflammatory processes caused by bacterial infection. Parathyroid hormone (PTH) plays a critical role in bone remodeling. The present study aimed to investigate the influences of PTH on human bone marrow mesenchymal stem cells (HBMSCs) pretreated with lipopolysaccharide (LPS). The proliferative ability was measured using cell counting kit-8 (CCK-8) and flow cytometry. The optimal concentrations of PTH and LPS were determined using alkaline phosphatase (ALP) activity assay, ALP staining, and Alizarin Red staining. Osteogenic differentiation was further assessed by quantitative reverse-transcription polymerase chain reaction (RT-qPCR), Western blot analysis, and immunofluorescence staining. PTH had no effects on the proliferation of HBMSCs. Also, 100 ng/ml LPS significantly inhibited HBMSC osteogenesis, while  $10^{-9}$  mol/l PTH was considered as the optimal concentration to reverse the adverse effects. Mechanistically, c-Jun N-terminal kinase (JNK) phosphorylation was activated by PTH in LPS-induced HBMSCs. SP600125, a selective inhibitor targeting JNK mitogen-activated protein kinase (MAPK) signaling, weakened the effects of PTH. Taken together, the findings revealed the role and mechanism of PTH and JNK pathway in promoting the osteogenic differentiation of LPS-induced HBMSCs, which offered an alternative for treating periodontal diseases.

## Introduction

Periodontitis is a group of chronic inflammatory processes characterized by uncoordinated immune-inflammatory reactions, which has become a common cause of tooth loss in adults [1]. So far, no effective strategies have been developed to treat periodontitis. Lipopolysaccharide (LPS), a cell wall component of Gram-negative bacteria, presents as a major nexus for virulence in the pathogenesis of periodontitis [2,3]. Human bone marrow mesenchymal stem cells (HBMSCs) obtained from human bone marrow play a key role in cell-based therapies due to their remarkable functional nature [4,5]. HBMSCs can maintain low anti-inflammatory properties under the undifferentiated state and exhibit better bone formation capability during osteoblastic differentiation [6–8]. However, the LPS-induced local inflammatory environment increases the secretion of inflammatory factors and up-regulates the oxidative stress level [9,10], leading to an inadequate biologic behavior of HBMSCs during differentiation.

\*These authors contributed equally to this work.

Received: 27 February 2021

Revised: 02 July 2021

Accepted: 03 August 2021

Accepted Manuscript Online:  
04 August 2021

Version of Record published:  
20 August 2021

Therefore, discovering desirable strategies to promote HBMSC osteogenesis against an inflammatory environment is urgently needed.

Parathyroid hormone (PTH), an endocrine factor secreted by the parathyroid gland, has significant effects in terms of regulating bone metabolism and has been used as the only approved therapy by the Food and Drug Administration for osteoporosis in the United States [11]. The secretion and synthesis of PTH are sensitively controlled by the calcium concentration detection mechanism. PTH exerts anabolic effects on both osteoblasts and osteocytes by regulating bone remodeling [12]. A previous study reported that PTH guided osteoblast lineage by influencing phenotypes through reducing cell apoptosis and increasing cell viability and differentiation potential [13]. Recent studies established that the intermittent delivery of PTH led to the up-regulated osteoblast activity and down-regulated osteoblast apoptosis in the bone marrow [14–16]. Nevertheless, the effects and the underlying mechanisms of PTH responsible for remodeling LPS-inhibited osteogenesis have not been fully elucidated yet. The activation of mitogen-activated protein kinase (MAPK) signals are involved in multiple physiological processes, including cell cycle control, apoptosis, and cell fate specification [17,18]. Moreover, MAPKs are often activated under inflammatory conditions, such as substances containing LPS [19]. Therefore, the present study was performed to investigate the role of PTH on the MAPK signaling pathway in LPS-induced HBMSCs.

The present study aimed to uncover the regulatory effects of PTH in the osteogenic differentiation of HBMSCs under inflammatory conditions. The role of c-Jun N-terminal kinase (JNK) MAPK was also evaluated. This might lay a foundation for the therapy of chronic inflammatory processes and expand the understanding of the impact of PTH on bone regeneration.

## Materials and methods

### HBMSC isolation, LPS treatment, and PTH administration

The present study was approved by the ethics committee of the Affiliated Hospital of Stomatology, Nanjing Medical University. The mandible samples of 80 patients, aged 20–30 years, treated by sagittal split ramus osteotomy (SSRO) in the Oral and Maxillofacial Surgery of the Affiliated Hospital of Stomatology, Nanjing Medical University were harvested. HBMSCs were isolated and cultured routinely, as reported in a previous study [20]. The isolated HBMSCs were maintained in Dulbecco's modified Eagle's medium (DMEM) (HyClone, U.S.A.) containing 10% fetal bovine serum (FBS; Gibco, Life Technologies), 100 U/l penicillin, and 100 µg/l streptomycin (Gibco). The cell culture was conducted in a humid environment with 5% CO<sub>2</sub> at 37°C. The medium was refreshed every 2 days, and the cells from three to six passages were used for the following experiments. HBMSCs ( $5 \times 10^4$  cells) were seeded on six-well culture plates (Corning). When the cell attachment reached 80%, HBMSCs were subjected to a 24-h treatment with serum-free medium or LPS (1 µg/ml) as previously described [21]. After 24 h, HBMSCs were washed with phosphate-buffered saline (PBS) and exposed to human PTH (1–34) (ApexBio, A1129). SP600125, a highly selective inhibitor of JNK signaling, was prepared in DMSO and used in the signaling inhibition assay. To eliminate the influence of SP600125 on PTH, LPS-induced HBMSCs were treated with SP600125 for 24 h after incubating in LPS before PTH treatment. All study protocols were approved by the ethics and research Committee of Nanjing Medical University. The permit number of the ethics committee is PJ2019-059-001. Informed consents were obtained from each participant.

### Cell proliferation assay

The cell proliferation was assessed using cell counting kit-8 (CCK-8) and flow cytometry. At the appointed time points, HBMSCs and HBMSCs treated with LPS or LPS + PTH were incubated with CCK-8 reagent (Dojindo, Kyushu Island, Japan) at 37°C for 2 h. The optical density (OD) was detected using a microplate reader (Bio-Tek, VT, U.S.A.) based on absorbance at 405 nm. Then, the cell cycle distribution (G<sub>0</sub>, G<sub>1</sub>, S, and G<sub>2</sub> M phases) was evaluated using an FACScan flow cytometer (BD Biosciences, U.S.A.) and quantitated using MODFIT LT 3.2 (Verity Software House, U.S.A.).

### Alkaline phosphatase activity assay and alkaline phosphatase staining

Osteogenic differentiation was induced in osteogenic media containing 100 nM dexamethasone, 10 mM β-glycerophosphate, and 100 nM ascorbic acid (Sigma Chemical Co., U.S.A.) for 7 days. Alkaline phosphatase (ALP) activity was detected using an ALP activity kit (Nanjing Jiancheng, Nanjing, China) based on the absorbance at 405 nm as previously reported [22]. Total protein was quantitated with a BCA kit (Beyotime, Shanghai, China), and the enzymatic activity was normalized by total cellular protein concentrations among the samples. For ALP staining, HBMSCs were fixed with 70% ethanol and stained using a BCIP/NBT ALP color development kit (Beyotime). The images were photographed under phase-contrast microscopy (Epson printer, Japan).

**Table 1 Primers employed for quantitative real-time reverse-transcription polymerase chain reaction**

Gene	Forward primer (5'–3')	Reverse primer (5'–3')
ALP	AGAACCCAAAGGCTTCTTC	CTTGGCTTTTCTTCATGGT
COL1	GGACACAATGGATTGCAAGG	TAACCACTGCTCCACTCTGG
OPN	CAGTTGTCCCCACAGTAGACAC	GTGATGTCTCGTCTGTAGCATC
OCN	AGCAAAGGTGCAGCCTTTGT	GCGCCTGGGTCTCTTCACT
RUNX2	TCTTAGAACAAATCTGCCCTTT	TGCTTTGGTCTTGAAATCACA
GAPDH	GAAGGTGAAGGTCGGAGTC	GAGATGGTGATGGGATTTC

## Alizarin Red staining

Osteogenic differentiation was induced for 14 days. The cells were fixed with 70% ethanol and stained with 2% Alizarin Red (pH = 4.2; Sigma, U.K.). The images were captured under a microscope (Epson printer).

## Quantitative real-time reverse-transcription polymerase chain reaction

The cellular RNA was extracted from cells using TRIzol reagent (Invitrogen, U.S.A.) and reverse transcribed using a reverse transcription kit (Applied Biosystems, CA, U.S.A.). Next, qRT-PCR was performed with SYBR Green Master Mix (Roche, Switzerland) on an ABI Prism 7500 real-time PCR system (Applied Biosystems) at 95°C for 30 s, followed by 40 cycles at 95°C for 5 s and 60°C for 31 s [23]. Table 1 summarizes the cDNA sequences, and GAPDH was employed as an internal reference. Data analysis was carried out by the  $2^{-\Delta\Delta C_t}$  method.

## Western blot analysis

Western blot analysis was carried out as previously reported [24]. Primary antibodies used were as follows: anti-runt-related transcription factor 2 (RUNX2) (#12556), ERK1/2 (#4695), anti-p-ERK1/2 (#4370), anti-JNK (#9252), anti-p-JNK (#9255), anti-p38 (#8690), anti-p-p38 (#4511), and anti- $\beta$ -actin (#3700) (Cell Signaling Technology, U.S.A.), anti-ALP (ab83259), anti-osteocalcin (OCN) (ab133612) (1:1000), anti-collagen 1 (COL1) (ab34710), and anti-osteopontin (OPN) (ab8448) (Abcam, U.K.) primary antibodies.  $\beta$ -actin served as an internal control. The relative densitometry analysis of the phosphorylation level was carried out using ImageJ software. The relative protein level was quantified as the ratio of the level of the target protein to the level of  $\beta$ -actin, in each group.

## Immunofluorescence

Immunofluorescence staining was carried out as previously reported [25]. After incubation with the primary antibodies [anti-OCN (1:200) and anti-Runx2 (1:500); Abcam, U.K.] at 4°C overnight, the cells were incubated with the following secondary antibody for 1 h: Alexa Fluor 594 (1/1000; Abcam, U.K.). The nuclei were counterstained with DAPI solution (Invitrogen). The images were visualized under an inverted fluorescence microscope (Olympus, Shanghai, China).

## Statistical analysis

The experiments were all carried out for at least three times. Representative data were displayed as mean  $\pm$  standard deviation (SD). SPSS 20.0 software (SPSS Inc., U.S.A.) was employed for data analysis. Differences between two groups were evaluated by the two-tailed Student's *t* test. ANOVA was used to determine significance between multiple groups. A *P*-value <0.05 indicated a statistically significant difference.

## Results

### Effects of LPS on the growth and osteogenic differentiation of HBMSCs

The flow cytometry analysis detected the S-phase checkpoint between the HBMSCs and LPS treatment groups (1, 10, 100, 1000, and 10000 ng/ml LPS). No obvious differences were found (Figure 1A). The CCK-8 assay also demonstrated that various LPS concentrations had no effects on cell growth (Figure 1B). ALP and Alizarin Red staining showed that the osteogenic differentiation in HBMSCs was gradually inhibited by increasing LPS concentrations. Further, 100 ng/ml LPS markedly reduced the ALP level and matrix mineralization, and no further changes were found in the 10000 ng/ml group (Figure 1C). Based on these findings, the concentration of 100 ng/ml LPS was selected as the optimal level to mimic the inflammatory environment.

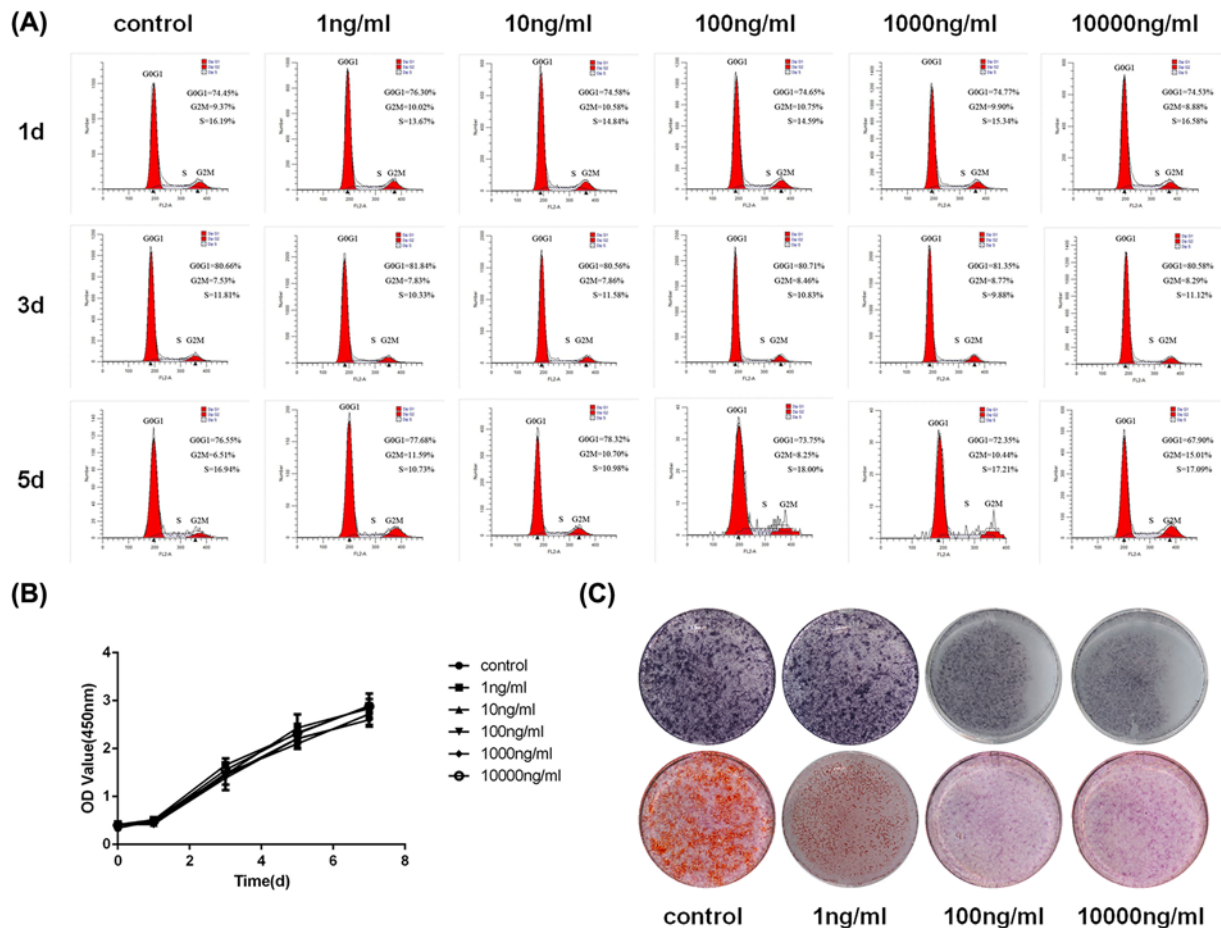


**Figure 1. LPS had no effects on proliferation and inhibited osteogenic differentiation of HBMSCs**

(A) Flow cytometry analysis showed no effects of liposomes on the cell cycle of HBMSCs after 1, 3, and 5 days. (B) Cell viability assessed by CCK-8 showed that LPS did not affect cell proliferation. (C) Osteogenic differentiation assessed by ALP staining and Alizarin Red staining was inhibited under the stimulation of 100 ng/ml LPS,  $n=5$ .

## Effects of PTH on LPS-induced HBMSC proliferation

PTH ( $10^{-7}$ ,  $10^{-9}$ ,  $10^{-11}$ , and  $10^{-13}$  M) was added to HBMSCs with LPS treatment. No significant differences were found in cell viability and S-phase population among the control, LPS, and LPS + PTH groups (Figure 2A,B). Therefore, PTH had no effects on the proliferative ability of LPS-induced HBMSCs.

## Screening for the optimal PTH concentration

After LPS treatment, HBMSCs were incubated with different concentrations of PTH ( $10^{-7}$ ,  $10^{-9}$ ,  $10^{-11}$ , and  $10^{-13}$  M). The  $10^{-9}$  M PTH group showed the most elevated ALP amounts compared with other PTH groups, as confirmed by ALP activity and staining (Figure 3A,B). Meanwhile, Alizarin Red staining demonstrated that matrix mineralization was the highest in the  $10^{-9}$  M PTH group, while other PTH groups showed no differences compared with the LPS group (Figure 3C). These results suggested  $10^{-9}$  M as the optimal PTH level for evaluating osteogenic differentiation in LPS-induced HBMSCs.

## Effects of PTH on LPS-induced osteogenic differentiation of HBMSCs

The effect of  $10^{-9}$  M PTH on osteogenic differentiation in LPS-induced HBMSCs was further examined. ALP, COL1, OPN, OCN, and RUNX2 mRNA levels decreased on LPS administration, whereas PTH treatment resulted in opposite effects (Figure 4A). Meanwhile, Western blot analysis revealed that ALP, COL1, OPN, OCN, and RUNX2 protein levels were markedly lower in the LPS group than in the control group, while PTH reversed these inhibitory effects (Figure 4B). Besides, the expression of OCN and RUNX2 was obviously up-regulated in the PTH treatment group



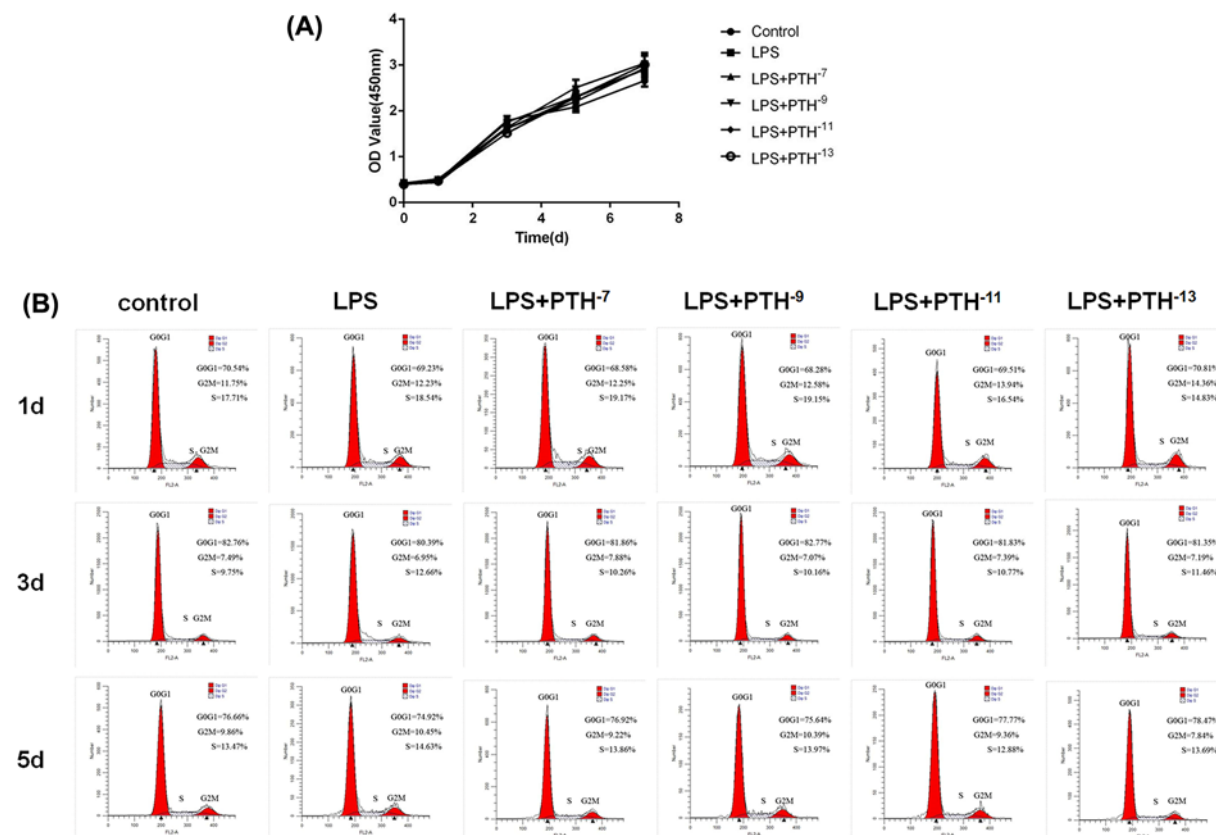


**Figure 2. PTH had no effects on LPS-induced HBMSC proliferation**

(A) Cell viability of HBMSCs assessed by CCK-8 showed that PTH did not affect cell proliferation. (B) Flow cytometry analysis showed no effects of PTH on the cell cycle of HBMSCs after 1, 3, and 5 days,  $n=5$ .

compared with the LPS group, as revealed by immunofluorescence (Figure 4C,D). Collectively, these results indicated that PTH enhanced the osteogenesis of LPS-induced HBMSCs.

## Role of the JNK MAPK pathway in PTH-induced osteogenesis

JNK, p-JNK, p38, p-p38, ERK1/2, and p-ERK1/2 protein levels were measured to investigate the role of MAPK signaling in PTH-associated processes. Compared with control untreated HBMSCs, LPS administration remarkably suppressed JNK phosphorylation. However, elevated p-JNK levels were detected in the PTH group compared with the LPS group, while p38, p-p38, ERK1/2, and p-ERK1/2 protein levels exhibited no distinct differences (Figure 5A). The ratio of p-JNK/JNK also indicated the activated JNK pathway after PTH treatment (Figure 5B). To further clarify the underlying mechanisms, SP600125, a specific inhibitor of JNK MAPK, was applied. SP600125 inhibited the beneficial effects of PTH in reversing JNK phosphorylation (Figure 5C). As expected, SP600125 reduced ALP activity and ALP-positive area driven by PTH (Figure 6A,B). Besides, Alizarin Red staining and qRT-PCR demonstrated that the mineralization and osteogenic gene expression levels driven by PTH were remarkably reduced on SP600125 administration (Figure 6B,C). In addition, the protein levels of osteogenic markers enhanced by PTH also decreased after SP600125 administration (Figure 6D-F). So far, the results demonstrated that PTH promoted the osteogenic differentiation of LPS-induced HBMSCs through the JNK MAPK pathway.

## Discussion

Alveolar bone regeneration plays a key role in treating periodontitis. The osteogenic differentiation property of mesenchymal stem cells in an inflammatory environment is important during this process. Accumulating evidence indicates that LPS serves as an inflammatory factor and impairs the formation of a localized osteogenic microenvironment by penetrating the periodontal tissue [26–28]. HBMSCs, which exhibit the advantages of extensive sources and low

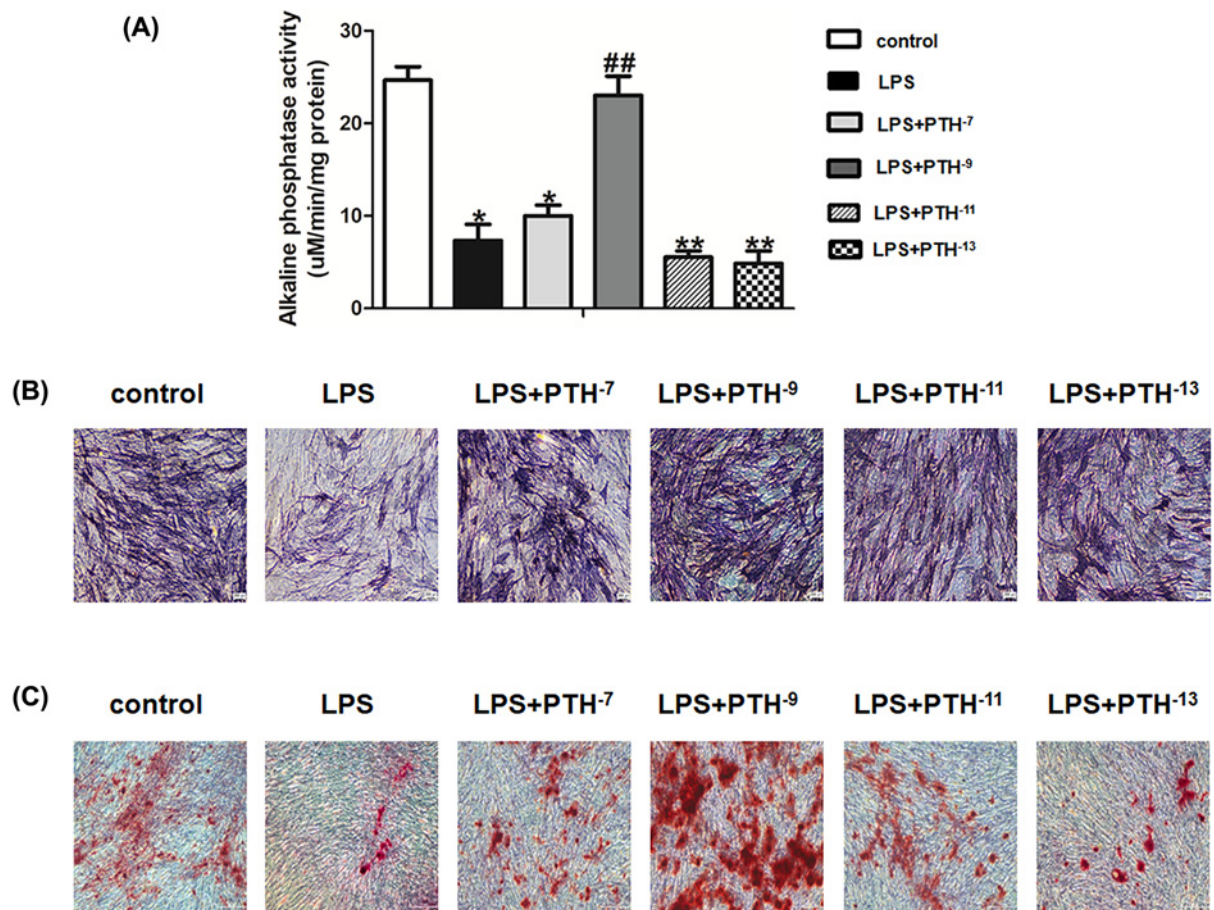


**Figure 3. A concentration of  $10^{-9}$  M as the optimal PTH level on osteogenic differentiation in LPS-induced HBMSCs**  
(A,B) ALP levels detected by ALP staining and activity assay showed that the concentration of PTH at which the osteogenic differentiation of HBMSCs was the strongest was  $10^{-9}$  M. (C) Matrix mineralization determined by Alizarin Red staining also indicated that  $10^{-9}$  M PTH was the best for osteogenic differentiation in LPS-induced HBMSCs. Data are mean  $\pm$  SD. \* $P < 0.05$  and \*\* $P < 0.01$  versus the control (HBMSCs) group; ## $P < 0.01$  versus the LPS (HBMSCs + LPS) group,  $n = 5$ . Scale bar, 200  $\mu$ m.

immunogenicity, are essential in alleviating bone complications [29]. Besides, HBMSCs also show considerable benefits in regenerating periodontal tissue according to their self-renewal and multiple differentiation properties [30]. Nevertheless, diminished osteogenesis, unexpected adipogenesis, and suppressed osteoblast-related gene expression have been reported in LPS-induced HBMSCs [31]. An inflammatory microenvironment formed by LPS was created to decrease the osteogenesis of HBMSCs in the present study, confirming previous findings [32]. Therefore, better strategies to reverse the inhibited osteogenic differentiation of HBMSCs might help design new approaches for treating periodontitis.

The influence of PTH on bone remodeling is well established [33]. PTH serves as an effective anabolic therapeutic in reducing the apoptosis and senescence of HBMSCs [34,35]. In addition, PTH also promotes HBMSC proliferation, maintains HBMSC integrity, and slows down age-related osteoporosis in adult mice by reversing HBMSC apoptosis [36]. Furthermore, daily injections of PTH result in a considerable increase in mass, strength, and mineral density of bone, contributing to the improvement in bone microarchitecture and healing of bone defect size [37]. We hypothesized that PTH could impede the pathophysiological processes in LPS-induced HBMSCs. First, we demonstrated that PTH did not affect the proliferative capacity of HBMSCs based on a series of experiments. Next, ALP staining and activity, qRT-PCR, and Western blot analysis indicated that  $10^{-9}$  M PTH was optimal in reversing ALP inhibition caused by LPS, which represented an early osteogenic marker during mineralization [38]. COL1 represents an important structural protein displaying excellent osteoconductive function [39]. OPN is a regulator with a dual role in bone metabolism [40]. OCN is considered a late-stage osteogenic marker, reflecting the mature osteogenesis phenotype [41]. RUNX2 is a transcription factor that acts as an early-stage osteogenic marker in regulating bone tissue

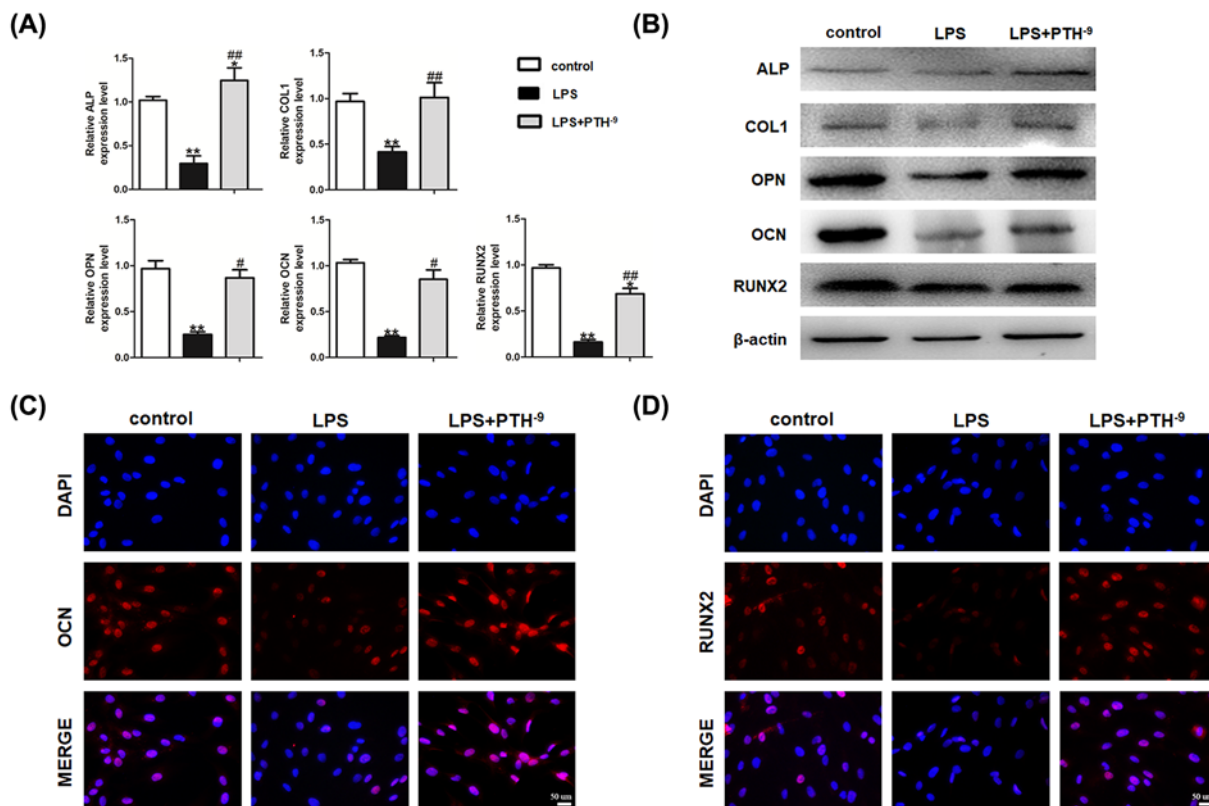


**Figure 4. PTH promoted osteogenesis in LPS-induced HBMSCs**

(A) Relative mRNA levels of ALP, COL1, OPN, OCN, and RUNX2 assessed by qRT-PCR suggested that PTH promoted osteogenesis-related gene expression. (B) Protein levels of ALP, COL1, OPN, OCN, and RUNX2, determined by Western blot analysis, also confirmed that the osteogenic ability of HBMSCs was elevated by PTH under the stimulation of LPS. (C,D) Expression levels of OCN and RUNX2 revealed by immunofluorescence were higher in the PTH (HBMSCs + LPS + PTH) group than in the LPS (HBMSCs + LPS) group. Data are mean  $\pm$  SD. \* $P$ <0.05 and \*\* $P$ <0.01 versus the control (HBMSCs) group; # $P$ <0.05 and ## $P$ <0.01 versus the LPS (HBMSCs + LPS) group,  $n$ =5. Scale bar, 50  $\mu$ m.

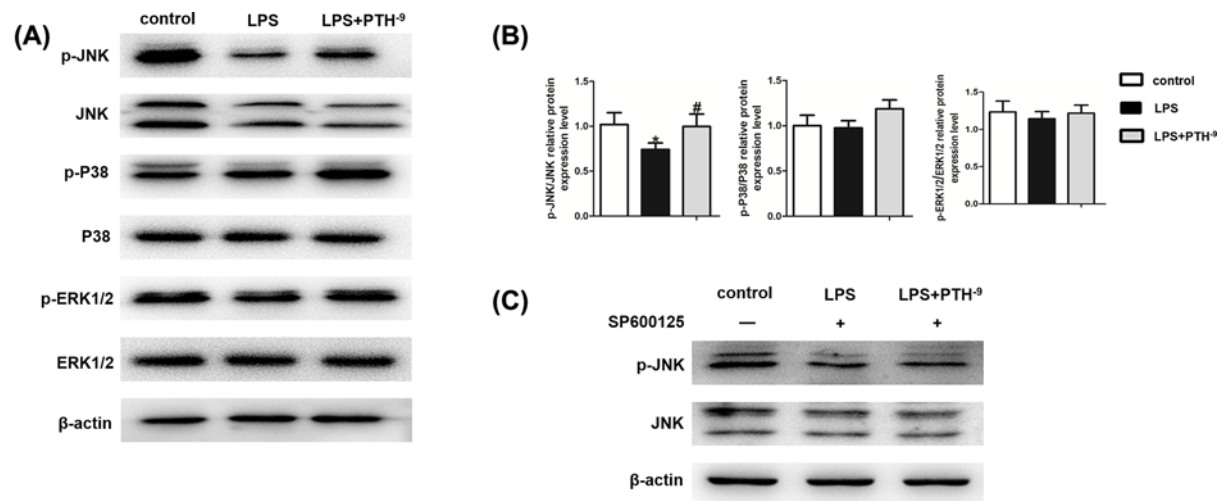


**Figure 5. Impact of PTH on the MAPK pathway**

(A) p-JNK, JNK, p-p38, p38, p-ERK1/2, and ERK1/2 protein levels assessed by Western blot analysis. The expression of p-JNK was elevated in the PTH group compared with the LPS group, while p38, p-p38, ERK1/2, and p-ERK1/2 protein exhibited no distinct differences. (B) Relative phosphorylation level was measured by densitometry analysis using ImageJ software. (C) Protein amounts of p-JNK and JNK obtained by Western blot analysis on SP600125 treatment showed that PTH increased the expression of p-JNK. Data are mean  $\pm$  SD. \* $P$ <0.05 versus the control (HBMSCs) group; # $P$ <0.05 versus the LPS (HBMSCs + LPS) group,  $n$ =5.



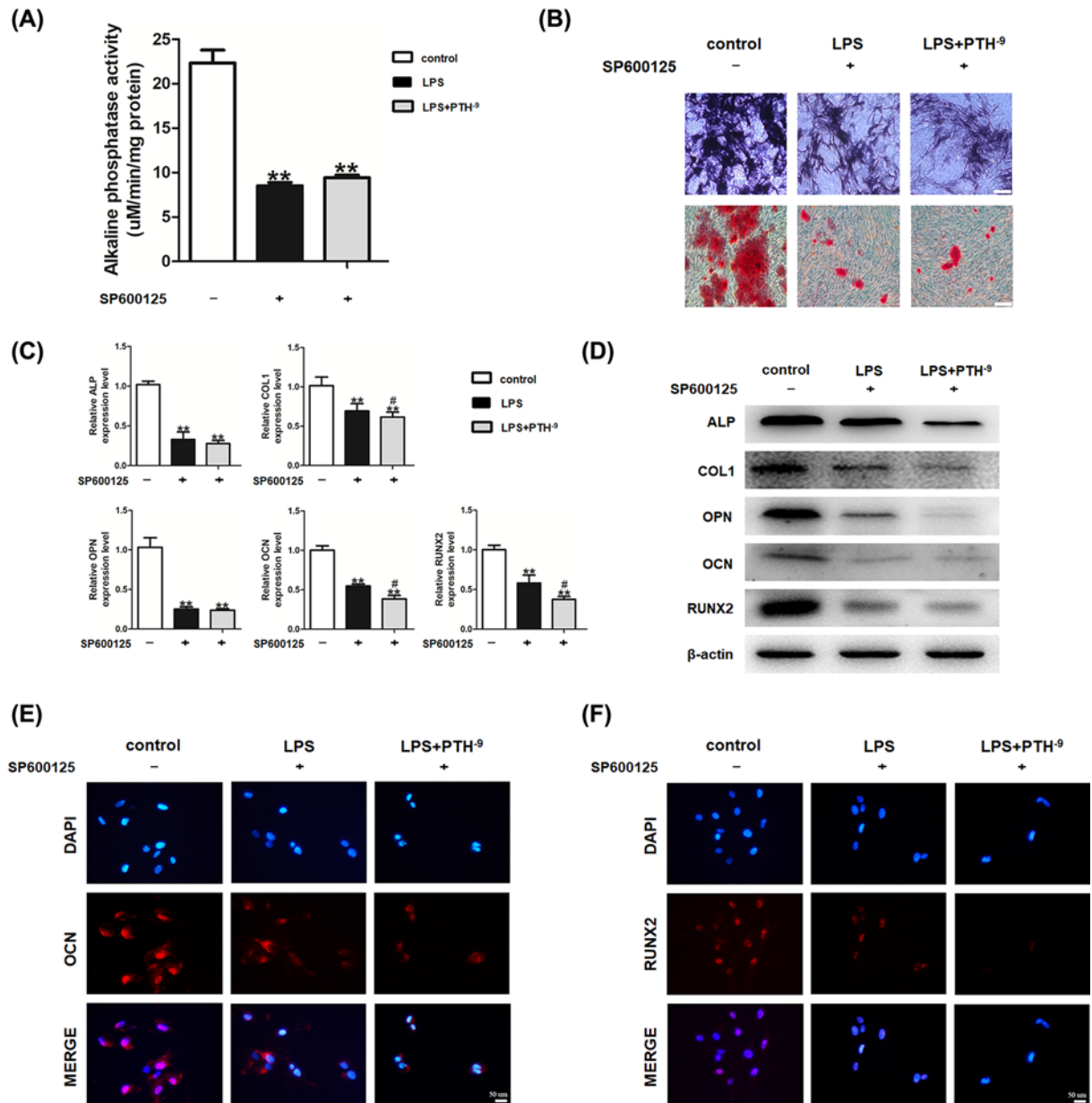


**Figure 6.** PTH promoted osteogenic differentiation by activating the JNK MAPK pathway

(A,B) ALP levels detected by ALP staining and activity assay; mineralized matrix formation assessed by Alizarin Red staining. SP600125, a specific inhibitor of JNK MAPK, depleted the osteogenic ability of PTH under LPS stimulation. Scale bar, 200  $\mu$ m. (C) Relative ALP, COL1, OPN, OCN, and RUNX2 mRNA amounts evaluated by qRT-PCR suggested that SP600125 reversed the promoting effects of PTH on osteogenesis-related gene expression. (D) Protein levels of ALP, COL1, OPN, OCN, and RUNX2, determined by Western blot analysis, indicated that the inhibition of JNK dampened the expression of osteogenesis-related proteins. (E,F) Expression levels of OCN and RUNX2 revealed by immunofluorescence were lower in the SP600125 (HBMSCs + LPS + PTH + SP600125) group than in the LPS (HBMSCs + LPS + SP600125) group. Scale bar, 50  $\mu$ m. Data are mean  $\pm$  SD. \*\* $P$ <0.01 versus the control (HBMSCs) group; # $P$ <0.05 versus the LPS (HBMSCs + LPS) group,  $n$ =5.

enrichment [42]. We further suggested that PTH rectified the inhibition of the aforementioned osteogenic markers by LPS. Based on Alizarin Red staining data, we concluded that PTH had a better effect in remodeling LPS-induced HBMSCs.

The MAPK pathway was closely associated with PTH treatment. MAPK is a broad-based protein kinase that acts as an indispensable part of signal transduction [43]. Three major subfamilies of MAPK (ERK1/2, JNK, and p38)



represent valuable triggers for the differentiation of mesenchymal stem cells [44]. As shown earlier, PTH elevated p-JNK levels in LPS-induced HBMSCs, highlighting the role of phosphorylated JNK in restoring bone deficiency. A specific pathway inhibitor was further applied, and the results confirmed that suppressing JNK MAPK significantly inhibited PTH-driven osteogenesis. Taken all these findings together, PTH promoted the osteogenic differentiation in HBMSCs against LPS through the JNK MAPK pathway.

In summary, these data uncovered a potential role for PTH in treating LPS-induced HBMSCs and provided novel insights into a potential strategy therapy of the inflammatory bone-destructive processes. Further *in vivo* experiments are needed to understand the detailed mechanisms better.

## Data Availability

The materials, data, and any associated protocols that support the findings of the present study are available from the corresponding authors upon request.

## Competing Interests

The authors declare that there are no competing interests associated with the manuscript.

## Funding

This work was supported by the Priority Academic Program Development of Jiangsu Higher Education Institutions (PAPD) [grant number 2018–87]; the National Natural Science Foundation of China [grant number 81800936]; the Natural Science Foundation of Jiangsu Province [grant numbers BK20180668, BK20190648]; the China Postdoctoral Science Foundation Funded Project [grant numbers 2018M64050, 2019T120445]; the Jiangsu Postdoctoral Science Foundation Funded Project [grant number 2018K251C]; the Jiangsu Province Undergraduate Innovation and Entrepreneurship Training Program [grant number 201910312004Z]; and the Open Research Fund of Jiangsu Key Laboratory of Oral Diseases [grant number JSKLOD-KF-1903].

## CRedit Author Contribution

**Ziyue Qin:** Formal analysis, Investigation, Writing—original draft. **Shu Hua:** Formal analysis, Investigation, Writing—original draft. **Huifen Chen:** Data curation, Software, Writing—review and editing. **Zhuo Wang:** Data curation, Software, Writing—review and editing. **Haoran Wang:** Data curation, Software, Writing—review and editing. **Jiamin Xu:** Data curation, Software, Writing—review and editing. **Yuli Wang:** Conceptualization, Resources. **Wu Chen:** Conceptualization, Resources. **Weina Zhou:** Conceptualization, Resources.

## Abbreviations

ALP, alkaline phosphatase; CCK-8, cell counting kit-8; COL1, collagen 1; DAPI, 4',6-diamidino-2-phenylindole; GAPDH, glyceraldehyde-3-phosphate dehydrogenase; HBMSC, human bone marrow mesenchymal stem cell; JNK, c-Jun N-terminal kinase; LPS, lipopolysaccharide; MAPK, mitogen-activated protein kinase; OCN, osteocalcin; OPN, osteopontin; PBS, phosphate-buffered saline; PTH, parathyroid hormone; RUNX2, runt-related transcription factor 2.

## References

- Pihlstrom, B.L., Michalowicz, B.S. and Johnson, N.W. (2005) Periodontal diseases. *Lancet North Am. Ed.* **366**, 1809–1820
- Uehara, A. and Takada, H. (2007) Functional TLRs and NODs in human gingival fibroblasts. *J. Dent. Res.* **86**, 249–254
- Beutler, B. and Rietschel, E.T. (2003) Innate immune sensing and its roots: the story of endotoxin. *Nat. Rev. Immunol.* **3**, 169–176
- Bruder, S.P., Jaiswal, N. and Haynesworth, S.E. (1997) Growth kinetics, self-renewal, and the osteogenic potential of purified human mesenchymal stem cells during extensive subcultivation and following cryopreservation. *J. Cell. Biochem.* **64**, 278–294
- Augello, A. and De Bari, C. (2010) The regulation of differentiation in mesenchymal stem cells. *Hum. Gene Ther.* **21**, 1226–1238
- Inoue, K., Ohgushi, H., Yoshikawa, T., Okumura, M., Sempuku, T., Tamai, S. et al. (1997) The effect of aging on bone formation in porous hydroxyapatite: biochemical and histological analysis. *J. Bone Miner. Res.* **12**, 989–994
- Le Blanc, K., Tammik, L., Sundberg, B., Haynesworth, S.E. and Ringden, O. (2003) Mesenchymal stem cells inhibit and stimulate mixed lymphocyte cultures and mitogenic responses independently of the major histocompatibility complex. *Scand. J. Immunol.* **57**, 11–20
- Miura, M., Miura, Y., Padilla-Nash, H.M., Molinolo, A.A., Fu, B., Patel, V. et al. (2006) Accumulated chromosomal instability in murine bone marrow mesenchymal stem cells leads to malignant transformation. *Stem Cells* **24**, 1095–1103
- Islam, S., Hassan, F., Turmurkhuu, G., Dagvadorj, J., Koide, N., Naiki, Y. et al. (2007) Bacterial lipopolysaccharide induces osteoclast formation in RAW 264.7 macrophage cells. *Biochem. Biophys. Res. Commun.* **360**, 346–351
- Mormann, M., Thederan, M., Nackchbandi, I., Giese, T., Wagner, C. and Hansch, G.M. (2008) Lipopolysaccharides (LPS) induce the differentiation of human monocytes to osteoclasts in a tumour necrosis factor (TNF) alpha-dependent manner: a link between infection and pathological bone resorption. *Mol. Immunol.* **45**, 3330–3337

- 11 Chandra, A., Lan, S., Zhu, J., Lin, T., Zhang, X., Siclari, V.A. et al. (2013) PTH prevents the adverse effects of focal radiation on bone architecture in young rats. *Bone* **55**, 449–457
- 12 Li, J.Y., D'Amelio, P., Robinson, J., Walker, L.D., Vaccaro, C., Luo, T. et al. (2015) IL-17A is increased in humans with primary hyperparathyroidism and mediates PTH-induced bone loss in mice. *Cell Metab.* **22**, 799–810
- 13 Esen, E., Lee, S.Y., Wice, B.M. and Long, F. (2015) PTH promotes bone anabolism by stimulating aerobic glycolysis via IGF signaling. *J. Bone Miner. Res.* **30**, 2137
- 14 Jilka, R.L., Weinstein, R.S., Bellido, T., Roberson, P., Parfitt, A.M. and Manolagas, S.C. (1999) Increased bone formation by prevention of osteoblast apoptosis with parathyroid hormone. *J. Clin. Invest.* **104**, 439–446
- 15 Kaback, L.A., Soung do, Y., Naik, A., Geneau, G., Schwarz, E.M., Rosier, R.N. et al. (2008) Teriparatide (1–34 human PTH) regulation of osterix during fracture repair. *J. Cell. Biochem.* **105**, 219–226
- 16 Yang, C., Frei, H., Burt, H.M. and Rossi, F. (2009) Effects of continuous and pulsatile PTH treatments on rat bone marrow stromal cells. *Biochem. Biophys. Res. Commun.* **380**, 791–796
- 17 Hu, Y., Chan, E., Wang, S.X. and Li, B. (2003) Activation of p38 mitogen-activated protein kinase is required for osteoblast differentiation. *Endocrinology* **144**, 2068–2074
- 18 Suzanne, M., Irie, K., Glise, B., Agnes, F., Mori, E., Matsumoto, K. et al. (1999) The Drosophila p38 MAPK pathway is required during oogenesis for egg asymmetric development. *Genes Dev.* **13**, 1464–1474
- 19 Yeom, M., Kim, J.H., Min, J.H., Hwang, M.K., Jung, H.S. and Sohn, Y. (2015) Xanthii fructus inhibits inflammatory responses in LPS-stimulated RAW 264.7 macrophages through suppressing NF-kappaB and JNK/p38 MAPK. *J. Ethnopharmacol.* **176**, 394–401
- 20 Akintoye, S.O., Lam, T., Shi, S., Brahim, J., Collins, M.T. and Robey, P.G. (2006) Skeletal site-specific characterization of orofacial and iliac crest human bone marrow stromal cells in same individuals. *Bone* **38**, 758–768
- 21 Jung, W.K., Park, I.S., Park, S.J., Yea, S.S., Choi, Y.H., Oh, S. et al. (2009) The 15-deoxy-Delta12,14-prostaglandin J2 inhibits LPS-stimulated AKT and NF-kappaB activation and suppresses interleukin-6 in osteoblast-like cells MC3T3E-1. *Life Sci.* **85**, 46–53
- 22 Ge, W., Shi, L., Zhou, Y., Liu, Y., Ma, G.E., Jiang, Y. et al. (2011) Inhibition of osteogenic differentiation of human adipose-derived stromal cells by retinoblastoma binding protein 2 repression of RUNX2-activated transcription. *Stem Cells* **29**, 1112–1125
- 23 Yan, M., Wu, J., Yu, Y., Wang, Y., Xie, L., Zhang, G. et al. (2014) Mineral trioxide aggregate promotes the odonto/osteogenic differentiation and dentinogenesis of stem cells from apical papilla via nuclear factor kappa B signaling pathway. *J. Endod.* **40**, 640–647
- 24 Ge, X., Li, Z., Jing, S., Wang, Y., Li, N., Lu, J. et al. (2020) Parathyroid hormone enhances the osteo/odontogenic differentiation of dental pulp stem cells via ERK and P38 MAPK pathways. *J. Cell. Physiol.* **235**, 1209–1221
- 25 Ouyang, N., Li, H., Wang, M., Shen, H., Si, J. and Shen, G. (2020) The transcription factor Foxc1 promotes osteogenesis by directly regulating Runx2 in response of intermittent parathyroid hormone (1–34) treatment. *Front. Pharmacol.* **11**, 592
- 26 Guo, C., Yuan, L., Wang, J.G., Wang, F., Yang, X.K., Zhang, F.H. et al. (2014) Lipopolysaccharide (LPS) induces the apoptosis and inhibits osteoblast differentiation through JNK pathway in MC3T3-E1 cells. *Inflammation* **37**, 621–631
- 27 Guo, C., Wang, S.L., Xu, S.T., Wang, J.G. and Song, G.H. (2015) SP600125 reduces lipopolysaccharide-induced apoptosis and restores the early-stage differentiation of osteoblasts inhibited by LPS through the MAPK pathway in MC3T3-E1 cells. *Int. J. Mol. Med.* **35**, 1427–1434
- 28 Wang, Y., Wu, H., Shen, M., Ding, S., Miao, J. and Chen, N. (2017) Role of human amnion-derived mesenchymal stem cells in promoting osteogenic differentiation by influencing p38 MAPK signaling in lipopolysaccharide -induced human bone marrow mesenchymal stem cells. *Exp. Cell. Res.* **350**, 41–49
- 29 Jing, H., Su, X., Gao, B., Shuai, Y., Chen, J., Deng, Z. et al. (2018) Epigenetic inhibition of Wnt pathway suppresses osteogenic differentiation of BMSCs during osteoporosis. *Cell Death Dis.* **9**, 176
- 30 Gu, C., Xu, Y., Zhang, S., Guan, H., Song, S., Wang, X. et al. (2016) miR-27a attenuates adipogenesis and promotes osteogenesis in steroid-induced rat BMSCs by targeting PPARgamma and GREM1. *Sci. Rep.* **6**, 38491
- 31 Xing, Q., Ye, Q., Fan, M., Zhou, Y., Xu, Q. and Sandham, A. (2010) Porphyromonas gingivalis lipopolysaccharide inhibits the osteoblastic differentiation of preosteoblasts by activating Notch1 signaling. *J. Cell. Physiol.* **225**, 106–114
- 32 Ochi, H., Hara, Y., Tagawa, M., Shinomiya, K. and Asou, Y. (2010) The roles of TNFR1 in lipopolysaccharide-induced bone loss: dual effects of TNFR1 on bone metabolism via osteoclastogenesis and osteoblast survival. *J. Orthop. Res.* **28**, 657–663
- 33 Caplan, A.I. (1991) Mesenchymal stem cells. *J. Orthop. Res.* **9**, 641–650
- 34 Geng, S., Zhou, S. and Glowacki, J. (2011) Age-related decline in osteoblastogenesis and 1alpha-hydroxylase/CYP27B1 in human mesenchymal stem cells: stimulation by parathyroid hormone. *Aging Cell* **10**, 962–971
- 35 Yu, B., Zhao, X., Yang, C., Crane, J., Xian, L., Lu, W. et al. (2012) Parathyroid hormone induces differentiation of mesenchymal stromal/stem cells by enhancing bone morphogenetic protein signaling. *J. Bone Miner. Res.* **27**, 2001–2014
- 36 Jilka, R.L., Almeida, M., Ambrogini, E., Han, L., Roberson, P.K., Weinstein, R.S. et al. (2010) Decreased oxidative stress and greater bone anabolism in the aged, when compared to the young, murine skeleton with parathyroid hormone administration. *Aging Cell* **9**, 851–867
- 37 Harris, S.E., Rediske, M., Neitzke, R. and Rakian, A. (2017) Periodontal biology: stem cells, Bmp2 Gene, transcriptional enhancers, and use of sclerostin antibody and Pth for treatment of periodontal disease and bone loss. *Cell Stem Cells Regen. Med.* **3**, 1–12
- 38 Halling Linder, C., Ek-Rylander, B., Krumpel, M., Norgard, M., Narisawa, S., Millan, J.L. et al. (2017) Bone alkaline phosphatase and tartrate-resistant acid phosphatase: potential co-regulators of bone mineralization. *Calcif. Tissue Int.* **101**, 92–101
- 39 Mushahary, D., Wen, C., Kumar, J.M., Lin, J., Harishankar, N., Hodgson, P. et al. (2014) Collagen type-I leads to in vivo matrix mineralization and secondary stabilization of Mg-Zr-Ca alloy implants. *Colloids Surf. B Biointerfaces* **122**, 719–728
- 40 Uaesoontrachoon, K., Yoo, H.J., Tudor, E.M., Pike, R.N., Mackie, E.J. and Pagel, C.N. (2008) Osteopontin and skeletal muscle myoblasts: association with muscle regeneration and regulation of myoblast function in vitro. *Int. J. Biochem. Cell Biol.* **40**, 2303–2314

- 41 Phimphilai, M., Zhao, Z., Boules, H., Roca, H. and Franceschi, R.T. (2006) BMP signaling is required for RUNX2-dependent induction of the osteoblast phenotype. *J. Bone Miner. Res.* **21**, 637–646
- 42 Phillips, J.E., Gersbach, C.A., Wojtowitz, A.M. and Garcia, A.J. (2006) Glucocorticoid-induced osteogenesis is negatively regulated by Runx2/Cbfa1 serine phosphorylation. *J. Cell Sci.* **119**, 581–591
- 43 Hu, N., Feng, C., Jiang, Y., Miao, Q. and Liu, H. (2015) Regulative effect of Mir-205 on osteogenic differentiation of bone mesenchymal stem cells (BMSCs): possible role of SATB2/Runx2 and ERK/MAPK pathway. *Int. J. Mol. Sci.* **16**, 10491–10506
- 44 Qin, L., Tang, B., Deng, B., Mohan, C., Wu, T. and Peng, A. (2015) Extracellular regulated protein kinases play a key role via bone morphogenetic protein 4 in high phosphate-induced endothelial cell apoptosis. *Life Sci.* **131**, 37–43